INT. J. RADIAT. BIOL 2001, VOL. 77, NO. 2, 155–164

DNA strand break yields after post-high LET irradiation incubation with endonuclease-III and evidence for hydroxyl radical clustering

J. R. MILLIGAN†*, J. A. AGUILERA†, R. A. PAGLINAWAN†, J. F. WARD† and C. L. LIMOLI‡

(Received 9 August 2000; accepted 10 October 2000)

Abstract.
Purpose: To determine the increase in single- (SSB) and double-strand break (DSB) yields after post-high LET irradiation incubation of plasmid DNA with the endonuclease-III (endo-III) of *Escherichia coli*.
Materials and methods: Plasmid DNA in aerobic aqueous solution was irradiated with one of five radiation types: ^{137}Cs γ-rays (LET ~ 0.3 keV μm^{-1}), ^{244}Cm α-particles (140–190 keV μm^{-1}), ^{4}He ions (97 keV μm^{-1}), ^{56}Fe ions (143 keV μm^{-1}) or ^{197}Au ions (1440 keV μm^{-1}). The irradiated samples were then incubated with endo-III. SSB and DSB yields were quantified by agarose gel electrophoresis.
Results: Endo-III incubation produced an increase in the SSB and DSB yields. The increases were in general lower after the high LET irradiation than after γ-irradiation. This may reflect inhibition of the activity of endo-III by the nearby DNA damage expected from high LET radiation. It can be shown that even if the activity of endo remains unchanged, significantly lower increases in SSB and DSB yields would still be expected.
Conclusion: The results provide evidence for clustered DNA damage after high LET irradiation.

1. Introduction

It is widely accepted that DNA damage plays a central role in the biological effects of ionizing radiation. One type of damage, the DNA double-strand break (DSB), is correlated with the lethal effects of irradiation. Some effort has been devoted to understanding the relationship (Blakely 1992) between the linear energy transfer (LET) of the radiation and its relative biological effectiveness (RBE) in terms of the yields and types of DSB involved. The general conclusion is that the biological consequences are a much stronger function of the complexity than of the number of DSB (Goodhead 1995). Models of energy deposition by ionizing radiation suggest that the energy deposition events are not evenly distributed in space, and that this distribution is increasingly non-random with increasing LET (Nikjoo *et al.* 1998). After allowing for the limited diffusion of reactive intermediates from the particle track under cellular conditions (Nikjoo *et al.* 1999), the conclusion is that multiple chemical modifications of DNA are expected in regions having dimensions of the order of 10 nm. Because of the compact structural folding of DNA in chromatin (van Holde 1988), this physical distance (nominally equivalent to ~ 30 base pairs) may correspond to significantly larger distances when mapped along the DNA axis. There is experimental evidence to support the non-random distribution of DSB in cells subjected to high LET radiation (Löbrich *et al.* 1996, Newman *et al.* 1997).

Considerable effort has been devoted to identifying the nature and yield of the individual products of DNA damage introduced by ionizing radiation. These products include breaks in one or both strands (single-strand breaks, SSB, and DSB), and chemical modifications of the bases. The relative yields vary to some extent depending on the experimental conditions (e.g. single-or double-stranded DNA substrate, oxygen concentration), but the major products under aerobic conditions are SSB, the 8-oxo derivatives of guanine and adenine, an oxazolone product derived from guanine degradation, the formamidopyrimidines derived from guanine and adenine, and the glycols derived from thymine and cytosine (Fuciarelli *et al.* 1990, Swarts *et al.* 1996, Cadet *et al.* 1997b). There is some concern about the artefactual formation of some of these products (Cadet *et al.* 1997a). This concern is mainly restricted to low dose and *in vivo* situations where the products are formed in very low yield. Products containing two adjacent modified bases have also been detected (Box *et al.* 2000).

Biophysical models predict that DNA damage caused by ionizing radiation should include a significant contribution from multiple modifications caused by multiple reactive intermediates at the nanometer level (Ward 1981, Goodhead *et al.* 1994). The severity of this so-called clustered or multiple damage is expected to increase with increasing LET.

*Author for correspondence; e-mail: jmilligan@ucsd.edu
†Department of Radiology, University of California at San Diego, La Jolla, CA 92093-0610, USA and ‡Department of Radiation Oncology, University of California at San Francisco, San Francisco, CA 94103, USA.

International Journal of Radiation Biology ISSN 0955-3002 print/ISSN 1362-3095 online © 2001 Taylor & Francis Ltd
http://www.tandf.co.uk/journals
DOI: 10.1080/09553000010013445

Clustered damage is assumed to consist of collections of two or more of the individual products mentioned above (Ward 1994). The only combinations that are easily detected by commonly used assays are those involving two SSB in opposite strands located sufficiently close to one another to result in the formation of a DSB. In double-stranded DNA, SSB are formed from $^{\bullet}$OH with a yield of 11–12% (LaVerne and Pimblott 1993). It is therefore probable that DSB yields underestimate the yields of clustered damage.

Consequently it is desirable to detect base damage in close proximity to a SSB. In principle it is possible to do this by exploiting the activity of base excision repair enzymes. These endonucleases have the property of removing certain modified bases and then introducing SSB at the resulting abasic sites. The increase in the SSB yield after incubation with a base excision endonuclease provides an estimate of the yields of those modified bases that are its substrates (Epe and Hegler 1994). Depending upon the SSB assay, this may be significantly more sensitive than chromatographic methods. A post-incubation increase in the DSB yield provides a way to detect clustered damage involving a much wider range of DNA damage than just two SSB in complementary strands (Sutherland *et al.* 2000a, b). Here is reported the increases in the SSB and DSB yields after *E. coli* endonuclease-III (endo-III) incubation of plasmid DNA irradiated with γ-rays or one of four high LET particles.

2. Materials and methods

2.1. *Preparation of DNA substrate and* E. coli *endonuclease-III*

The procedures used for the preparation and purification of plasmid pEC (10.8 kb) have been described by Milligan *et al.* (1993). Endo-III of *E. coli* was generously provided by R. P. Cunningham, State University of New York at Albany. The purification procedures for endo-III have been described by Asahara *et al.* (1989).

2.2. *Plasmid DNA solution*

Solutions contained sodium phosphate (10^{-2} mol dm^{-3}, pH 7.0), sodium formate (10^{-4} mol dm^{-3}), and plasmid pEC at 1000 μg ml^{-1}. They were irradiated at room temperature in equilibrium with air. The $^{\bullet}$OH scavenging capacity of this solution is $\sim 3 \times 10^{5}$ s^{-1}, which corresponds to an $^{\bullet}$OH diffusion distance of $\sim$ 100 nm.

2.3. γ-*ray irradiation*

Aliquots of 5 μl were irradiated in 500 μl polypropylene tubes to one of 10 doses. The dose-rate (9.9×10^{-3} Gy s^{-1}) was determined with the Fricke system (Spinks and Woods 1976).

2.4. α-*Particle and* ^{4}*He ion irradiation*

Helium-4 ions and α-particles with kinetic energy in the 5–10 MeV range travel $\sim$ 50–100 μm in water. Special precautions are therefore required to ensure that the sample thickness is less than this value so that the entire sample is irradiated. Described previously was the use of chambers in the form of an annular steel ring 40 mm in diameter fitted at one end with a 6 μm-thick Mylar window (Jones *et al.* 1993). A 4.8 μl drop of the plasmid solution was placed on the Mylar membrane, and forced by the application of a glass cover slip to assume the form of a rectangular prism 22 mm square and therefore 10 μm thick. An additional drop of the solvent was placed on top of the cover slip, and the chamber sealed with Parafilm to prevent evaporation of the sample. These chambers were irradiated either with ^{4}He ions or α-particles.

Helium-4 ion irradiation was undertaken at the RARAF van de Graaff accelerator (Nevis Laboratory, Columbia University). Dosimetry involved an ionization chamber also fitted with a 6 μm-thick Mylar window. The LET was determined with a counter of 6 μm thickness again fitted with a 6 μm-thick Mylar window. These two devices were used to characterize the beam before and after the irradiation of several samples (typically 1 h apart). During irradiation, the dose-rate was assumed to be proportional to the beam current. The mean LET within the sample was 97 keV μm^{-1}, with dose-rates in the range 0.9–1.1 Gy s^{-1}.

For α-particle irradiation, the chambers were placed directly above an isotopic α-particle (5.8 MeV) source consisting of a circular disk 40 mm in diameter coated with ^{244}Cm (Isotope Products Laboratories, Burbank, CA, USA) and protected with a layer of gold (0.24 μm). The LET and particularly the dose-rate from the isotopic source are difficult to estimate with precision, because the α-particles are emitted isotropically by the source, and no precautions were taken to collimate them. By comparison with previous results, we have obtained with accelerated ^{4}He ions using identical chambers (Jones *et al.* 1993, Milligan *et al.* 1996a), and estimated the α-particle dose-rate to be of the order of 10^{-1} Gy s^{-1}. The Aldose software package (Turner and Huston 1991) suggests an LET range within the 10 μm sample of

140–190 keV μm^{-1}, after allowing for energy loss in the intervening gold and Mylar layers. Note that the absolute SSB and DSB yields for α-particle irradiation are unimportant, because we are principally concerned with relative yields (the ratio of after to before enzyme incubation; see Discussion).

2.5. *Heavy ion (Fe and Au) irradiation*

Iron ($^{56}Fe^{26+}$) and gold ($^{197}Au^{79+}$) ion irradiation was provided at the Alternating Gradient Synchrotron (AGS) at Brookhaven National Laboratory (Zeitlin *et al.* 1998). Aliquots (10 μl) of the plasmid solution were irradiated in 0.5 ml polypropylene tubes placed in the path of the ion beam. For Fe ions, the kinetic energy was 1.1 GeV per nucleon for a dose average LET = 143 keV μm^{-1} (with ~10% of the dose deposited at lower values by fragmentation products) at a dose-rate of $\sim 2.5 \times 10^{-2}$ Gy s^{-1} (determined with three ionization chambers upstream of the sample during the irradiation). For Au ions, the corresponding values are kinetic energy = 11 GeV per nucleon, LET = 1400 keV μm^{-1} and dose-rate = $\sim 7 \times 10^{-4}$ Gy s^{-1}.

2.6. *Enzyme incubation*

After irradiation, samples were incubated with endo-III. Control incubations in the absence of any added enzyme were also included. The DNA solutions were diluted by a factor of 10 to a DNA concentration of 100 μg ml^{-1} with a solution containing tris(hydroxymethyl)aminomethane (Tris, 10^{-2} mol dm^{-3}, pH 8.0) and sodium chloride (10^{-1} mol dm^{-3}), and then 1 μg (i.e. 10 μl) aliquots were incubated for 30 min at 37°C with 1 μl of a solution containing endo-III at one of several concentrations (1–5 μg ml^{-1}). The enzyme reaction was halted by dilution with a loading buffer and followed immediately by electrophoresis. To minimize experimental errors, unirradiated aliquots of DNA solutions that had been irradiated with one of the four high LET particles (^{244}Cm α-particles, $^{4}He^{2+}$ ions, $^{56}Fe^{26+}$ ions, $^{197}Au^{97+}$ ions) were also subjected to γ-rays, and both of these samples were incubated with aliquots of the same diluted solution of the enzyme at the same time.

2.7. *Electrophoresis and determination of SSB and DSB yields*

These procedures have been described by Jones *et al.* (1993) and Milligan *et al.* (1996a).

3. Results

3.1. *SSB yield dose plot*

Figure 1 shows the results of two typical experiments. In these two cases, plasmid pEC was irradiated with either γ-rays or Fe ions. In both cases, as the radiation dose increases, the fraction of supercoiled (SSB free) plasmids decreases. In both cases, incubation of the plasmid after irradiation but before electrophoresis results in a more rapid loss with dose of the supercoiled form. It is possible to estimate radiation chemical yields (G) for SSB formation (hereafter G(SSB)) from the slopes of the straight lines fitted to the data in yield dose plots of the form of figure 1 (Milligan *et al.* 1993). G(SSB) for incubation in the absence of endo-III is denoted by G_0(SSB). For the γ-irradiation results plotted in figure 1, $G_0(SSB) = 5.98 \times 10^{-2}$ μmol J^{-1} and $G(SSB) = 1.14 \times 10^{-1}$ μmol J^{-1}; for the Fe ion irradiation, $G_0(SSB) = 1.16 \times 10^{-2}$ μmol J^{-1} and $G(SSB) = 1.82 \times 10^{-2}$ μmol J^{-1}.

The factor by which the yield of breaks increases as a result of endo-III is equal to the ratio $G(SSB)/G_0(SSB)$. From the data in figure 1, this factor is equal to $1.14 \times 10^{-1}/5.98 \times 10^{-2} = 1.91$ for γ-irradiation, and to $1.82 \times 10^{-2}/1.16 \times 10^{-2} = 1.57$ for Fe ion irradiation. In the absence of endo-III incubation, the SSB yield for Fe ions is lower than that for γ-rays by a factor of $5.98 \times 10^{-2}/1.16 \times 10^{-2} = 5.2$.

3.2. *DSB yield dose plot*

Figure 2 shows the formation of the linear form of the plasmid under the same conditions as figure 1. The fraction of linear plasmid increases with increasing radiation dose. This increase is greater after incubation with endo-III. In the same manner as for figure 1, the slopes of the straight lines fitted to the data in figure 2 can be used to estimate the G values for DSB formation (hereafter G(DSB)). G(DSB) after incubation in the absence of endo-III is symbolized by G_0(DSB). For γ-irradiation, $G_0(DSB) = 1.45 \times 10^{-3}$ mol J^{-1} and $G(DSB) = 4.82 \times 10^{-3}$ μmol J^{-1}; for the Fe ion irradiation, $G_0(DSB) = 4.61 \times 10^{-4}$ μmol J^{-1} and $G(DSB) = 9.86 \times 10^{-4}$ μmol J^{-1}.

The factor by which the yield of breaks increases as a result of endo-III is equal to the ratio $G(DSB)/G_0(DSB)$. From the data in figure 2, for γ-irradiation this factor is equal to $4.82 \times 10^{-3}/1.45 \times 10^{-3} = 3.32$, while for Fe ion irradiation it is equal to $9.86 \times 10^{-4}/4.61 \times 10^{-4} = 2.14$. In the absence of endo-III incubation, the DSB yield for Fe ions is lower than that for γ-rays by a factor of $1.45 \times 10^{-3}/4.61 \times 10^{-4} = 3.1$.

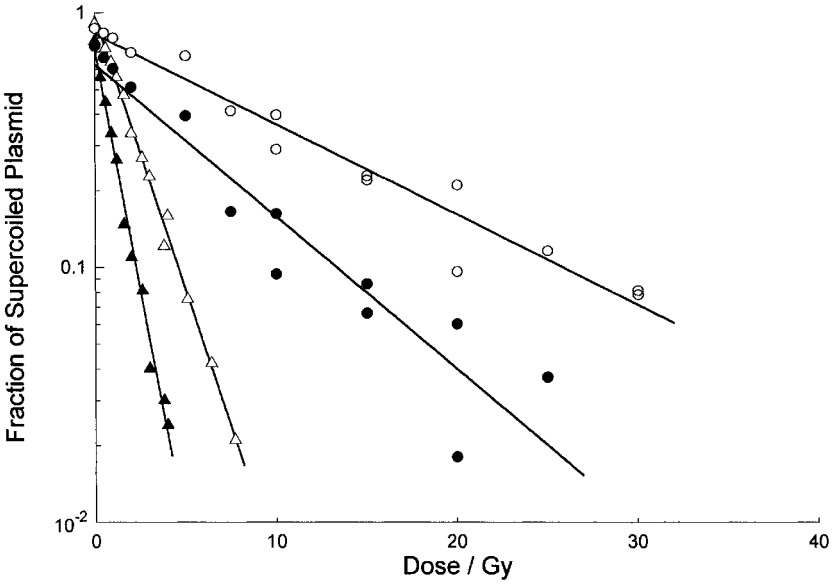

Figure 1. Loss of supercoiled plasmid DNA with increasing radiation dose. Plasmid pEC in the presence of 10^{-4} mol dm^{-3} sodium formate in equilibrium with air was irradiated with either ^{137}Cs γ-rays (triangles) or with $^{56}Fe^{26+}$ ions (circles) to the doses indicated, and then incubated either with (100 μg ml^{-1}, closed symbols) or without endo-III (open symbols). The fraction of intact supercoiled plasmid DNA remaining after each dose and each incubation was determined by agarose gel electrophoresis. The four data sets were fitted with least-mean-square straight lines of the form $y = ce^{-mx}$. From the slopes m of these lines, D_0 and SSB yields are: γ-ray without endo-III (open triangle), 2.02 Gy (5.98×10^{-2} μmol J^{-1} or 5.98×10^{-8} Gy^{-1} Da^{-1}); γ-ray and endo-III (closed triangle), 1.15 Gy (1.14×10^{-1} μmol J^{-1} or 1.14×10^{-7} Gy^{-1} Da^{-1}); $^{56}Fe^{26+}$ ion without endo-III (open circle), 12.3 Gy (1.16×10^{-2} μmol J^{-1} or 1.16×10^{-8} Gy^{-1} Da^{-1}); $^{56}Fe^{26+}$ ion and endo-III (closed circle), 7.30 Gy (1.82×10^{-2} μmol J^{-1} or 1.82×10^{-8} Gy^{-1} Da^{-1}).

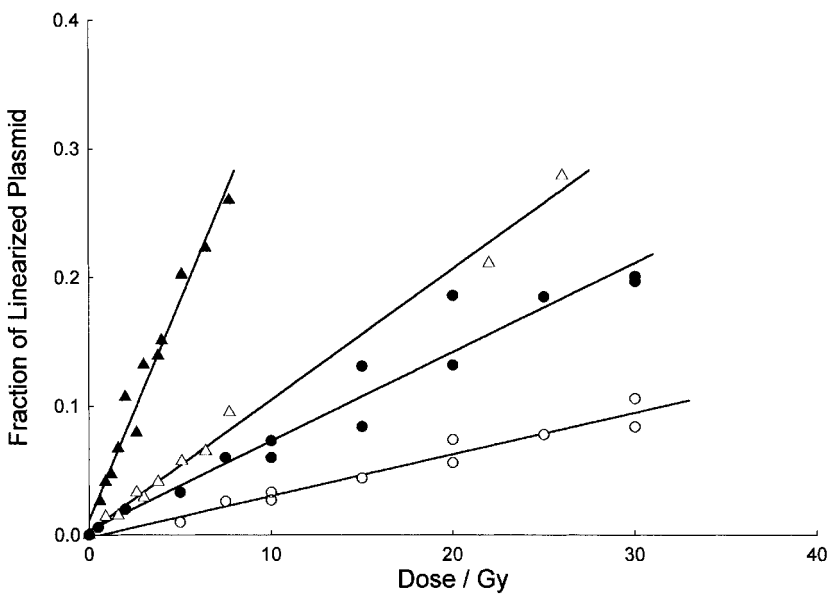

Figure 2. Formation of linearized plasmid DNA with increasing radiation dose corresponding to the loss of supercoiled plasmid shown in figure 1 (the experimental conditions were identical). The fraction of linear plasmid was also determined by agarose gel electrophoresis. The four data sets (symbols are identical) are fitted with least-mean-square second-order polynomials of the form $y = ax^2 + bx + c$. From b (slope of a tangent to the line at zero dose), the DSB yields are be calculated as: γ-ray without endo-III (open triangle), 1.21×10^{-3} μmol J^{-1} or 1.21×10^{-9} Gy^{-1} Da^{-1}; γ-ray and endo-III (closed triangle), 4.74×10^{-3} μmol J^{-1} or 4.74×10^{-9} Gy^{-1} Da^{-1}; $^{56}Fe^{26+}$ ion without endo-III (open circle), 4.67×10^{-4} μmol J^{-1} or 4.67×10^{-10} Gy^{-1} Da^{-1}; $^{56}Fe^{26+}$ ion and endo-III (closed circle), 9.98×10^{-4} μmol J^{-1} or 9.98×10^{-10} Gy^{-1} Da^{-1}.

Using the methods described above for figures 1 and 2, SSB and DSB yields were determined after irradiation under one of four conditions (α-particles, He ions, Fe ions, Au ions) followed by incubation with different concentrations of endo-III. The SSB and DSB yields determined after incubation in the absence of endo-III are listed in table 1 for γ-rays, He ions, Fe ions and Au ions. Absolute yields could not be determined for the isotopic α-particle source because of uncertainties in the dose-rate.

3.3. *Increase in the SSB yield*

In figure 3, $G(\mathrm{SSB})/G_0(\mathrm{SSB})$ for each of the four particles is plotted against $G(\mathrm{SSB})/G_0(\mathrm{SSB})$ for γ-rays. The values plotted against each other were determined at the same concentration of endo-III. For example, the values obtained from figure 1 require a symbol (open circle) for Fe ions with coordinates of 1.91 on the *x*-axis and 1.57 on the *y*-axis. For irradiation under any given set of conditions, higher concentrations of endo-III generally result in higher $G(\mathrm{SSB})/G_0(\mathrm{SSB})$ (Milligan *et al.* 1996). As $G(\mathrm{SSB})/G_0(\mathrm{SSB})$ (for γ-rays) increases from 1.3 to 2.4, $G(\mathrm{SSB})/G_0(\mathrm{SSB})$ (for the high LET particles) increases to a slightly lower extent from 1.1 to 1.9. These values are consistent with those determined by Prise *et al.* (1999) for γ- and α-irradiation under more efficiently scavenged conditions, followed by endo-III incubation. Also plotted in figure 3 are three curved lines representing the expected variation of the ratio $G(\mathrm{SSB})/G_0(\mathrm{SSB})$ for three particular multiply-damaged sites (MDS) as a function of $G(\mathrm{SSB})/G_0(\mathrm{SSB})$ for γ-rays (see Discussion).

Table 1. SSB and DSB yields after irradiation of plasmid pEC or pHAZE.

Radiation type	LET (keV μm^{-1})	G(SSB) (Gy^{-1} Da^{-1})	G(DSB) (Gy^{-1} Da^{-1})
γ-ray	≈0.3	5.98×10^{-8}	1.45×10^{-9}
$^{4}He^{2+}$	97	8.66×10^{-10}	1.07×10^{-10}
$^{56}Fe^{26+}$	145	1.16×10^{-8}	4.67×10^{-10}
$^{197}Au^{79+}$	1440	1.81×10^{-8}	3.83×10^{-10}

3.4. *Increase in the DSB yield*

In figure 4, $G(\mathrm{DSB})/G_0(\mathrm{DSB})$ for each of the four particles is plotted against $G(\mathrm{SSB})/G_0(\mathrm{SSB})$ for γ-rays, again where these values were determined at identical endo-III concentrations. Again as an example, the values obtained from figures 1 and 2 require a symbol for Fe ions at 1.91 on the *x*-axis (as in figure 3), and 2.14 on the *y*-axis. DSB data for γ-rays is also plotted in figure 4 for the purposes of comparison, but note we have reported previously on the relationship between the increases in the SSB and DSB yields for γ-rays over a wider range of both irradiation and incubation conditions (Milligan *et al.* 2000). For γ-irradiation, increases in the ratio $G(\mathrm{SSB})/G_0(\mathrm{SSB})$ from 1.1 to 2.2 correlate with increases in the $G(\mathrm{DSB})/G_0(\mathrm{DSB})$ ratio of 1.1 to 4.2 (~ 2-fold greater). For all four of the high LET particles, as the ratio $G(\mathrm{SSB})/G_0(\mathrm{SSB})$ increases from 1.3 to 2.4, the ratio

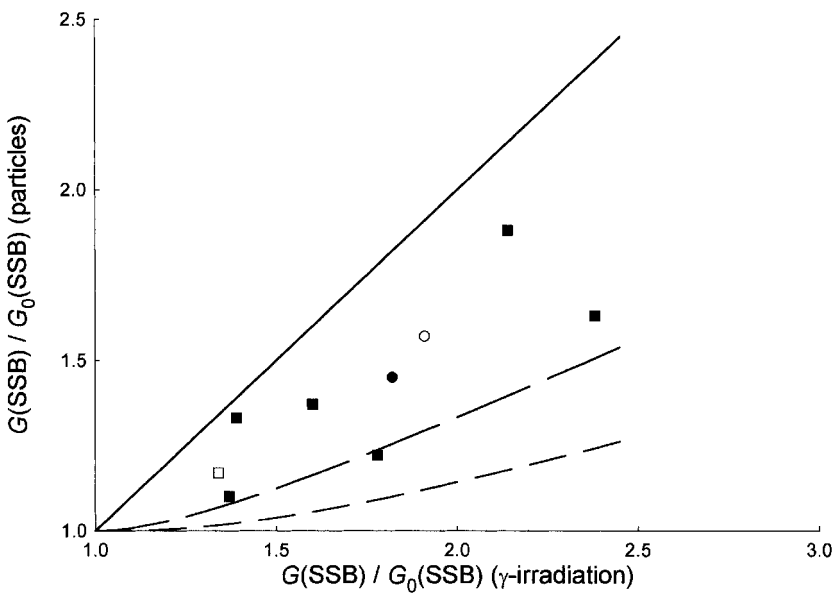

Figure 3. Correlation of increases in the SSB yields after post-irradiation endo-III incubation. The four different particles used were α-particles (closed square), He ions (open square), Fe ions (open circle) and Au ions (closed circle). Lines represent the expected correlations for MDS of the form 1:0 (solid line), 2:0 (long dash) and 3:0 (short dash). See the Discussion for details.

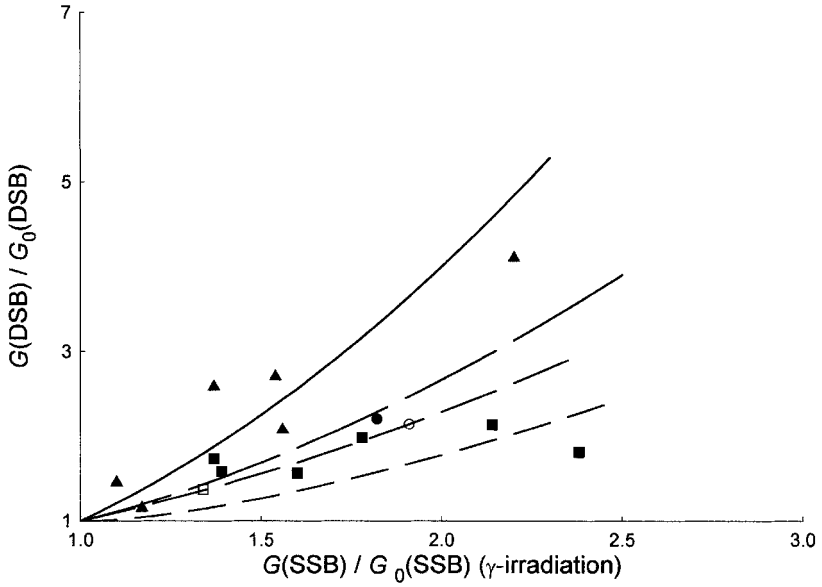

Figure 4. Correlation of increases in DSB yields with increases in SSB yields. The four different particles used were α-particles (closed square), He ions (open square), Fe ions (open circle) and Au ions (closed circle). γ-ray data (closed triangle) are also included. Lines represent the expected correlations for MDS of the form 1:1 (solid line), 2:1 (long dash), 3:1 (medium dash) and 2:2 (short dash). See the Discussion for details.

G(DSB)/G_0(DSB) increases from 1.3 to 2.3 (i.e. by about the same factor). Again, these values are consistent with the observations of Prise *et al.* (1999) at higher scavenging capacities. Four curved lines are also plotted in figure 4. They represent the expected relationships between G(DSB)/G_0(DSB) for MDS of four particular types and G(SSB)/G_0(SSB) for γ-rays (see Discussion).

The reason for plotting the ratio G/G_0 for SSB and DSB yields obtained with the particles against the ratio G/G_0 for γ-ray SSB (figures 3 and 4) is that the γ-ray SSB data provide a convenient benchmark for comparison. When plotted in this way, the effect of endo-III activity is removed and it is the differences between the radiation types that is emphasized.

SSB and DSB yields after incubation in the absence of any added endo-III are collected in table 1. Because of the dependence of the $^{\bullet}$OH yield on scavenging capacity, LET and particle type (LaVerne 1989a, b), it is difficult to compare the SSB yields with Fe and Au ions in table 1 with far more extensive data in the literature (Taucher-Scholz and Kraft 1999). The ^{4}He ion results are consistent with those reported for low scavenging capacities (Jones *et al.* 1993, Milligan *et al.* 1996a).

4. Discussion

4.1. *Scavenging capacity*

The hydroxyl radical ($^{\bullet}$OH) scavenging capacity ($\sigma(^{\bullet}OH)$) used for these experiments was relatively low (10^{-4} mol dm^{-3} formate, equivalent to an $^{\bullet}$OH diffusion distance of ~100 nm). These conditions are unrepresentative of biological systems, where the intracellular diffusion distance is ~30-fold lower (Roots and Okada 1975). However, the very high doses required at higher scavenging capacities (essential to decrease the diffusion distance) could not be delivered by the AGS (Fe and Au ions) or by the ^{244}Cm source (α-particles) during exposure times that were remotely practical. Similar difficulties with low particle fluxes have also been reported by others in the field (Taucher-Scholz and Kraft 1999).

4.2. *SSB caused by γ-irradiation*

In this discussion the individual products in DNA that result from attack by a single $^{\bullet}$OH are referred to as lesions. A lesion is an individual strand break or an individual damaged or chemically modified base. It is well recognized that multiple lesions caused by ionizing radiations may be present in close proximity. Such lesions are commonly described as being clustered, or as constituting a MDS. It is possible to arrive at an estimate of the composition of a MDS by consideration of the ratios G(SSB)/G_0(SSB) and G(DSB)/G_0(DSB).

Because of the presence of various damaged bases, the SSB yield after enzyme incubation, G(SSB), is greater than the SSB yield in the absence of enzyme incubation, G_0(SSB). The amount by which G(SSB) is greater than G_0(SSB) is equal to the yield of enzyme

sensitive lesions (ESL, damaged bases which are recognized by endo-III). The ESL yield which is measured experimentally depends on: (1) the yields of the modified bases that are recognized as substrates by endo-III (Dizdaroglu *et al.* 1993); and also (2) on the activity of endo-III (Milligan *et al.* 1996b). The yields of these bases are assumed to be a fixed fraction of the $^{\bullet}$OH yield, and therefore also of G(SSB). Therefore at any given enzyme activity, the yield of ESL is equal to G(SSB) multiplied by some factor F. Factor F depends only on endo-III concentration (although see Section 4.6), with $F=0$ in the absence of any endo-III. We have previously shown that as the enzyme activity is increased to the level where breaks start to be introduced non-specifically (i.e. in unirradiated plasmid), the ratio G(SSB)/G_0(SSB) increases to a maximum of $\sim$2.5 for endo-III (Milligan *et al.* 1996b). This is consistent with the yields of oxidized bases in γ-irradiated aqueous DNA solutions as determined by GC-MS (Swarts *et al.* 1996) and the known substrate specificity of endo-III (Dizdaroglu *et al.* 1993). The total yield of breaks measured after enzyme incubation includes the breaks present before incubation, so that the relationship between G(SSB) and G_0(SSB) is given by

$$G(\mathrm{SSB}) = G_0(\mathrm{SSB}) + F \times G_0(\mathrm{SSB}) \quad (1)$$

Rearranging this to calculate the ratio plotted in figures 3 and 4

$$G(\mathrm{SSB})/G_0(\mathrm{SSB}) = F + 1 \quad (2)$$

We wish to compare this ratio for SSB yields caused by γ-irradiation with that for both SSB and DSB caused by α-particle irradiation. In this way we can interpret the results plotted in figures 3 and 4.

4.3. *DSB caused by γ-irradiation*

We have previously reported on the effect of endo-III incubation on DSB formation by γ-irradiation (Milligan *et al.* 2000). At the risk of repetition, the situation is discussed again here in slightly different terms because it is a special case that helps to clarify the situation for the effect of endo-III incubation on SSB and DSB formation under the higher LET conditions associated with particle irradiation.

An expression for the ratio G(DSB)/G_0(DSB) for γ-irradiation may be derived as follows. Assume that a DSB is formed by two $^{\bullet}$OH attacks, one on each of the two complementary strands. Such a MDS may be represented by the symbol '1:1'. There are three possibilities to consider for a 1:1 MDS: (1) a SSB is formed in both cases; (2) a SSB is formed in one strand, and an ESL is formed in the other strand; or (3) two ESL are formed. The second possibility occurs with twice the probability of the other two, so its contribution must be doubled to account for this. The DSB yield in the absence of enzyme incubation is again G_0(DSB). The DSB yield after enzyme incubation, G(DSB), will be greater than this because of the contributions made by the MDS containing one or two ESL. Assuming that the two $^{\bullet}$OH attacks are independent of one another, then the yield of MDS containing one SSB and one ESL is equal to the yield of MDS containing two SSB (i.e. the DSB yield before enzyme incubation) multiplied by the same factor F as would be the case if the SSB site in the complementary strand were not present, i.e. $F \times G_0$(DSB). The yield of MDS containing two ESL is therefore equal to $F^2 \times G_0$(DSB). Therefore, the total DSB yield after enzyme incubation is equal to

$$G(\mathrm{DSB}) = G_0(\mathrm{DSB}) + 2 \times F \times G_0(\mathrm{DSB}) + F^2 \times G_0(\mathrm{DSB}) \quad (3)$$

Again, on rearranging this expression to calculate the ratio plotted in figure 4

$$G(\mathrm{DSB})/G_0(\mathrm{DSB}) = 1 + 2F + F^2 \quad (4)$$

Comparison of equations (2) and (4) reveals for a 1:1 MDS that (at any given enzyme activity) the expected increase in the DSB yield is the square of the increase in the SSB yield (i.e. $(1+F)^2 = 1 + 2F + F^2$). We have reported previously that this is supported by experimental evidence (Milligan *et al.* 2000).

4.4. *SSB caused by high LET radiation*

High LET radiation is expected to give rise in the region of the particle track to a very high local $^{\bullet}$OH density, and there may be a significant contribution to SSB formation by lesions containing more than one damaged site.

Consider the case of a MDS containing two lesions in the same strand, designated by '2:0'. Again, as with the 1:1 MDS, there are three possibilities: (1) both damaged sites are SSB; (2) one site is a SSB while the other is an ESL; and (3) both sites are ESL. Again, the contribution made by the second MDS must be multiplied by a factor of two. Because the two lesions are both in the same strand, the effect of these 2:0 MDS on the break yield after enzyme incubation is different from the 1:1 MDS. For the 2:0 MDS, the first two cases (in which at least one SSB is present before enzyme incubation) give rise to a SSB before enzyme incubation. After enzyme incubation, the contribution by the third site must also be included. Again assuming the $^{\bullet}$OH attacks to be independent of one another, we arrive at the

following expression for the SSB yields before (G_0(SSB)) and after (G(SSB)) enzyme incubation

$$G_0(\mathrm{SSB}) = G(2\ \mathrm{SSB}) + 2 \times F \times G(2\ \mathrm{SSB}) \quad (5)$$

$$G(\mathrm{SSB}) = G(2\ \mathrm{SSB}) + 2 \times F \times G(2\ \mathrm{SSB}) + F^2 \times G(2\ \mathrm{SSB}) \quad (6)$$

where G(2 SSB) is the (unknown) yield of MDS consisting of two SSB in the same strand. As before, what is required is an expression for the ratio G(SSB)/G_0(SSB), because this is what is plotted on the y-axis of figure 3. Dividing equation (6) by equation (5) produces

$$G(\mathrm{SSB})/G_0(\mathrm{SSB}) = (F^2 + 2F + 1)/(2F + 1) \quad (7)$$

By following a similar although lengthier argument, an estimate of the ratio G(SSB)/G_0(SSB) for a 3:0 MDS consisting of three individual lesions may be shown to be $(F^3 + 3F^2 + 3F + 1)/(3F^2 + 3F + 1)$. The missing F^3 term in the denominator represents the exclusion of the one MDS containing three ESL, since this is the only MDS which is not detected as a SSB before enzyme incubation. The general term for a n:0 MDS consisting of n lesions all in the same strand is therefore $[(F + 1)^n]/[(F + 1)^n - F^n]$. Similar expressions have been derived for the radioprotective effect of thiols (Michael *et al.* 1991, Milligan *et al.* 1996a), which also decreases with increasing LET. The G(SSB)/G_0(SSB) ratios are plotted in figure 3 as a function of the ratio G(SSB)/G_0(SSB) expected for γ-irradiation (i.e. as a function of $F + 1$, see Section 4.2) for $n = 1, 2, 3$.

As the endo-III concentration increases, F also increases. This is consistent with the observation that the ratio G(SSB)/G_0(SSB) (for any one type of radiation) increases with endo-III concentration (closed squares in figure 3). However, the essential point is that this effect of endo-III in increasing the SSB yield is predicted to become less pronounced as n (the number of lesions per cluster) increases. The general trend of these lines in figure 3 reveals that as the number of individually damaged lesions per MDS increases, there is a decrease in the ratio G(SSB)/G_0(SSB) expected after enzyme incubation.

4.5. *DSB caused by α-particle irradiation*

Expressions similar to equation (7) may be derived for MDS containing more than one lesion in one or both of the strands. These MDS result in DSB formation after (and possibly also before) enzyme incubation. For example, for a 2:1 MDS, the ratio of DSB after and before enzyme incubation is given by G(DSB)/G_0(DSB) = $(F + 1)^3/(2F + 1)$. The expressions for the two quadruply damaged sites 3:1 and 2:2 are respectively $(F + 1)^4/(3F^2 + 3F + 1)$ and $(F + 1)^4/(4F^2 + 4F + 1)$. Although the numerator would be $(F + 1)^{m+n}$, it is not clear what form is taken by the denominator in the general term for a m:n MDS. Together with the 1:1 MDS described above, the G(DSB)/G_0(DSB) ratios expected for 2:1, 3:1 and 2:2 MDS are plotted as a function of $F + 1$ in figure 4. The conclusion to be drawn from the lines plotted in figure 4 is much the same as the situation in figure 3. As the complexity of the damage increases, the lines plotted in figure 4 show that the increase in the DSB yield after endo-III incubation is expected to become less pronounced.

4.6. *Reactivity of endo-III with MDS*

The lines plotted in figures 3 and 4 can be compared with the experimental data in quantitative terms only if the normal excision and lyase activities of endo-III remain uninhibited by nearby lesions. These activities of endo-III have been examined for the lesion dihydrothymine in double stranded oligonucleotides containing a modified base, an abasic sites, or a break in the complementary strand (Chaudhry and Weinfeld 1995, Chaudhry and Weinfeld 1997, Harrison *et al.* 1998). A closely situated modified base produces a significant inhibition, while breaks have a smaller effect. The particular product dihydrothymine is not a major product of irradiation under aerobic conditions (Swarts *et al.* 1996). The major products that are substrates for endo-III are pyrimidine glycols (Dizdaroglu *et al.* 1993, Cadet *et al.* 2000). Nevertheless, these observations still indicate that the precise predictions made by the lines plotted in figures 3 and 4 should be regarded with some caution. In quantitative terms, these observations suggest that at identical endo-III concentrations, a lower value for F applies to MDS than to single lesions. Therefore, the assumption that F depends only on the endo-III concentration is not strictly valid.

Note, however, that any attenuation of the activity of endo-III at complex MDS would tend to decrease the ratios G(SSB)/G_0(SSB) and G(DSB)/G_0(DSB) observed with high LET particles when compared with the ratios for γ-irradiation. It has been shown above that such decreases are expected at complex MDS even if endo-III remains uninhibited. For this reason, it is argued that the decreases (compared with γ-irradiation) in G(SSB)/G_0(SSB) (figure 3) and particularly in G(DSB)/G_0(DSB) (figure 4) observed for several high LET radiations provide evidence for DNA damage that consists of multiple lesions, even at the relatively low scavenging capacity of 10^{-4}

mol dm^{-3} formate ($^{\bullet}OH$ diffusion distance of ~ 100 nm).

4.7. *Composition of MDS produced by high LET radiation*

The overall product distribution of singly damaged sites produced by the indirect effect of low-LET radiation can be determined by chromatography and simple break assays. It is generally agreed that the break yield per $^{\bullet}OH$ is $< 15\%$ (LaVerne and Pimblott 1993), with the remaining 85% being various modified bases. An MDS consists of multiple lesions, but these are distributed between just two complementary strands of DNA. Therefore the probability that at least one of the strands contains a lesion that is a break is greater than 15%, even though the product distribution that describes the individual lesions remains unaltered. The effect of endo-III in producing additional breaks must therefore decrease with increasing clustering (quantified by equations 4 and 7).

5. Conclusions

Irradiation of plasmid DNA produces both SSB and DSB. The yields of both types of break damage increase if the plasmid is incubated after irradiation with the *E. coli* base excision enzyme endo-III. This increase is attributed to the conversion of damaged bases into strand breaks. The increase in both SSB and DSB yields is less pronounced for four particle irradiations (5.8 MeV α-particles, 97 keV μm^{-1} $^{4}He^{2+}$ ions, 145 keV μm^{-1} $^{56}Fe^{26+}$ ions, 1440 keV μm^{-1} $^{197}Au^{79+}$ ions) than it is for γ-rays. Such an effect is expected for clustered DNA damage, both because of the combinatorial properties of multiple lesions, and also because closely situated lesions have been shown to have an inhibitory effect upon the activity of endo-III. The estimates of the cluster sizes (SSB with one to two damaged sites, and DSB with two to four damaged sites) are only approximate, but they are consistent with previous estimates based upon the competition between chemical fixation and repair (Milligan *et al.* 1996a).

Acknowledgements

Supported by USPHS grant CA-46295. The Radiological Research Accelerator Facility (RARAF) is an NIH supported Resource Center through grants RR-11623 (NCRR) and CA-37967 (NCI). We are grateful to S. Marino and G. Randers-Pehrson (Center for Radiological Research, Columbia University) for operating the RARAF van de Graaff, to L. Heilbronn and J. Miller (Life Sciences Division, Lawrence Berkeley National Laboratory) for the AGS ion beam dosimetry, and to R. Cunningham (Department of Biological Sciences, State University of New York at Albany) for a gift of endonuclease III.

References

ASAHARA, H., WISTORT, P. M., BANK, J. F., BAKERIAN, R. H. and CUNNINGHAM, R. P., 1989, Purification and characterization of *Escherichia coli* endonuclease III from the cloned *nth* gene. *Biochemistry*, **28,** 4444–4449.

BLAKELY, E. A., 1992, Cell inactivation by heavy charged particles. *Radiation and Environmental Biophysics*, **31,** 181–196.

BOX, H. C., PATRZYC, H. B., DAWIDZIK, J. B., WALLACE, J. C., FREUND, H. G., IJIMA, H. and BUDZINSKI, E. E., 2000, Double bass lesions in DNA X-irradiated in the presence or absence of oxygen. *Radiation Research*, **153,** 442–446.

CADET, J., BERGER, M., DOUKI, T. and RAVANAT, J.-L., 1997b, Oxidative damage to DNA: formation, measurement, and biological significance. *Reviews in Physiological and Biochemical Pharmacology*, **131,** 1–87.

CADET, J., BOURDAT, A.-G., D'HAM, C., DUARTE, V., GASPARUTTO, D., ROMIEU, A. and RAVANAT, J.-L., 2000, Oxidative base damage to DNA: specificity of base excision repair enzymes. *Mutation Research*, **462,** 121–128.

CADET, J., DOUKI, T. and RAVANAT, J.-L., 1997a, Artifacts associated with the measurement of oxidized DNA bases. *Environmental Health Perspectives*, **105,** 1034–1039.

CHAUDHRY, M. A. and WEINFELD, M., 1995, The action of *Escherichia coli* endonuclease III on multiply damaged sites in DNA. *Journal of Molecular Biology*, **249,** 914–922.

CHAUDHRY, M. A. and WEINFELD, M., 1997, Reactivity of human apurinic/apyrimidinic endonuclease and *Escherichia coli* exonuclease III with bistranded abasic sites in DNA. *Journal of Biological Chemistry*, **272,** 15 650–15 655.

DIZDAROGLU, M., LAVAL, J. and BOITEUX, S., 1993, Substrate specificity of the *Escherichia coli* endonuclease III: excision of thymine and cytosine derived lesions in DNA produced by radiation generated free radicals. *Biochemistry*, **32,** 12 105–12 111.

EPE, B. and HEGLER, J., 1994, Oxidative DNA damage: endonuclease fingerprinting. *Methods in Enzymology*, **234,** 122–131.

FUCIARELLI, A. F., WEGHER, B. J., BLAKELY, W. F. and DIZDAROGLU, M., 1990, Yields of radiation induced base products in DNA: effects of DNA conformation and gassing conditions. *International Journal of Radiation Biology*, **58,** 397–415.

GOODHEAD, D. T., 1994, Initial events in the cellular effects of ionizing radiations: clustered damage in DNA. *International Journal of Radiation Biology*, **65,** 7–17.

GOODHEAD, D. T., 1995, Molecular and cell models of biological effects of heavy ion radiation. *Radiation and Environmental Biophysics*, **34,** 67–72.

HARRISON, L., HATAHET, Z., PURMAL, A. A. and WALLACE, S. S., 1998, Multiply damaged sites in DNA: interactions with Escherichia coli endonucleases III and VIII. *Nucleic Acids Research*, **26,** 932–941.

JONES, G. G. D., MILLIGAN, J. R., WARD, J. F., CALABRO-JONES, P. M. and AGUILERA, J. A., 1993, Yield of strand breaks as a function of scavenger concentration and LET for SV40 irradiated with ^{4}He ions. *Radiation Research*, **136,** 190–196.

LAVERNE, J. A., 1989a, Radical and molecular yields in the

radiolysis of water with carbon ions. *Radiation Physics and Chemistry International Journal of Radiation Applications and Instrumentation, Part C*, **34,** 135–143.

LAVERNE, J. A., 1989b, The production of OH radicals in the radiolysis of water with ^{4}He ions. *Radiation Research*, **118,** 201–210.

LAVERNE, J. A. and PIMBLOTT, S. M., 1993, Yields of hydroxyl radical and hydrated electron scavenging reactions in aqueous solutions of biological interest. *Radiation Research*, **135,** 16–23.

LÖBRICH, M., RYDBERG, B. and COOPER, P. K., 1996, Non-random distribution of DNA double strand breaks induced by particle irradiation. *International Journal of Radiation Biology*, **70,** 493–503.

MICHAEL, B. D., PRISE, K. M., FAHEY, R. C. and FOLKARD, M., 1991, Radical multiplicity in radiation induced DNA strand breaks: implications for their chemical modification. In E. M. Fielden and P. O'Neill *The Early Effects of Radiation on DNA* (New York: Springer), **54,** pp. 333–346.

MILLIGAN, J. R., AGUILERA, J. A. and WARD, J. F., 1993, Variation of single strand break yield with scavenger concentration for plasmid DNA irradiated in aqueous solution. *Radiation Research*, **133,** 151–157.

MILLIGAN, J. R., AGUILERA, J. A., WU, C. C. L., NG, J. Y.-Y. and WARD, J. F., 1996a, The difference that linear energy transfer makes to precursors of DNA strand breaks. *Radiation Research*, **145,** 442–448.

MILLIGAN, J. R., AGUILERA, J. A., NGUYEN, T.-T. D., PAGLINAWAN, R. A. and WARD, J. F., 2000, DNA strand breaks yields after post irradiation incubation with base excision repair endonucleases implicate hydroxyl radical pairs in double strand break formation. *International Journal of Radiation Biology* (in press).

MILLIGAN, J. R., NG, J. Y.-Y., WU, C. C. L., AGUILERA, J. A., WARD, J. F., KOW, Y. W., WALLACE, S. S. and CUNNINGHAM, R. P., 1996b, Methylperoxyl radicals as intermediates in the damage to DNA irradiated in aqueous dimethyl sulfoxide with gamma rays. *Radiation Research*, **146,** 436–443.

NEWMAN, H. C., PRISE, K. M., FOLKARD, M. and MICHAEL, B. D., 1997, DNA double strand break distributions in X-ray and α-particle irradiated V79 cells: evidence for non-random breakage. *International Journal of Radiation Biology*, **71,** 347–363.

NIKJOO, H., O´NEILL, P., TERRISSOL, M. and GOODHEAD, D. T., 1999, Quantitative modelling of DNA damage using Monte Carlo track structure method. *Radiation and Environmental Biophysics*, **38,** 31–38.

NIKJOO, H., UEHARA, S., WILSON, W. E., HOSHI, M. and GOODHEAD, D. T., 1998, Track structure in radiation biology. *International Journal of Radiation Biology*, **73,** 355–364.

PRISE, K. M., PULLAR, C. H. L. and MICHAEL, B. D., 1999, A study of endonuclease III sensitive sites in irradiated DNA: detection of alpha particle induced oxidative damage. *Carcinogenesis*, **20,** 905–909.

ROOTS, R. and OKADA, S., 1975, Estimation of life times and diffusion distances of radicals involved in X-ray induced strand breaks and killing of mammalian cells. *Radiation Research*, **64,** 306–320.

SPINKS, J. W. T. and WOODS, R. J., 1976, *An Introduction to Radiation Chemistry*, 2nd edn (New York: Wiley).

SUTHERLAND, B. M., BENNETT, P. V., SIDORKINA, O. and LAVAL, J., 2000a, Clustered damages and total lesions induced in DNA by ionizing radiation: oxidized bases and strand breaks. *Biochemistry*, **39,** 8026–8031.

SUTHERLAND, B. M., BENNETT, P. V., SIDORKINA, O. and LAVAL, J., 2000b, Clustered DNA damages induced in isolated DNA and in human cells by low doses of ionizing radiation. *Proceedings of the National Academy of Sciences, USA*, **97,** 103–108.

SWARTS, S. G., SMITH, G. S., MIAO, L. and WHEELER, K. T., 1996, Effects of formic acid hydrolysis on the quantitative analysis of radiation induced DNA base damage products assayed by gas chromatography/mass spectrometry. *Radiation and Environmental Biophysics*, **35,** 41–53.

TAUCHER-SCHOLZ, G. and KRAFT, G., 1999, Influence of radiation quality on the yield of DNA strand breaks in SV40 DNA irradiated in solution. *Radiation Research*, **151,** 595–604.

TURNER, J. E. and HUSTON, T. E., 1991, Aldose. A computer code to calculate absorbed dose rate, dose equivalent rate, and dose weighted LET as functions of depth in water irradiated by an α-particle disc source. *Health Physics*, **60,** 581–585.

VAN HOLDE, K. E., 1988, *Chromatin* (New York: Springer).

WARD, J. F., 1981, Some biochemical consequences of the spatial distribution of ionizing radiation produced free radicals. *Radiation Research*, **86,** 185–195.

WARD, J. F., 1994, The complexity of DNA damage—relevance to biological consequences. *International Journal of Radiation Biology*, **66,** 427–432.

ZEITLIN, C., HEILBRONN, L. and MILLER, J., 1998, Detailed characterization of the 1087 MeV/nucleon iron-56 beam used for radiobiology at the alternating gradient synchrotron. *Radiation Research*, **149,** 560–569.